Physica B 407 (2012) 3278–3281

Contents lists available at SciVerse ScienceDirect

Physica B

journal homepage: www.elsevier.com/locate/physb

Adsorption of fluids on solid surfaces: A route toward very dense layers

S.A. Sartarelli [a], L. Szybisz [b,c,d,*]

[a] Instituto de Desarrollo Humano, Universidad Nacional de General Sarmiento, San Miguel, Argentina
[b] Laboratorio TANDAR, Departamento de Física, Comisión Nacional de Energía Atómica, RA-1429 Buenos Aires, Argentina
[c] Departamento de Fiica, Facultad de Ciencias Exactas y Naturales, Universidad de Buenos Aires, Argentina
[d] Consejo Nacional de Investigaciones Científicas y Técnicas, RA-1033 Buenos Aires, Argentina

ARTICLE INFO

Available online 19 December 2011

Keywords:
Wetting
Structure of simple liquids
Liquid–vapor transitions

ABSTRACT

Adsorption of Xe on single planar walls is investigated in the frame of a density functional theory. The strength of the adsorbate-substrate attraction is changed by considering surfaces of Cs, Na, Li, and Mg. The behavior is analyzed by varying the temperature T (between the triple point T_t and the critical T_c) and the coverage Γ_ℓ. The obtained adsorption isotherms exhibit a variety of wetting situations. Density profiles are reported. It is shown that for strongly attractive surfaces the adsorbed liquid becomes very dense reaching densities characteristic of solids.

1. Introduction

Since several decades the study of adsorption of fluids on solid walls is a topic of considerable interest. An entire volume devoted to reviews and discussions of specific theoretical as well as experimental investigations on this subject was recently published [1]. From that set of articles arises that properties of systems involving fluids at interfaces are not only interesting from the fundamental physics point of view, but have also numerous technological applications. Main features of adsorption are primarily determined by the ratio of the strength of the surface–fluid attraction, W_{sf}, and the well depth of the fluid–fluid interaction, ε_{ff}. In the present work, we describe how the first layer of a given fluid adsorbed on a single wall evolves from a standard liquid density to a very dense matter when $\epsilon_r = W_{sf}/\varepsilon_{ff}$ is increased.

The calculations have been carried out in the frame of the density functional (DF) formalism recently applied for studying physisorption of Ne and Ar [2–4]. In such a theory the Helmholtz free energy $F_{\rm DF}$ of a fluid embedded in an external potential $U_{sf}(\mathbf{r})$ is expressed as a functional of $\rho(\mathbf{r})$

$$F_{\rm DF}[\rho(\mathbf{r})] = \nu_{\rm id} k_B T \int d\mathbf{r}\, \rho(\mathbf{r})\{\ln[\Lambda^3\rho(\mathbf{r})]-1\}$$

$$+ \int d\mathbf{r}\, \rho(\mathbf{r})\Delta f_{\rm HS}[\overline{\rho}(\mathbf{r}); d_{\rm HS}] + \frac{1}{2}\iint d\mathbf{r}\, d\mathbf{r}'$$

$$\times \rho(\mathbf{r})\rho(\mathbf{r}')\Phi_{\rm attr}(|\mathbf{r}-\mathbf{r}'|) + \int d\mathbf{r}\, \rho(\mathbf{r})U_{sf}(\mathbf{r}). \quad (1)$$

The first term is the ideal gas free energy, where k_B is the Boltzmann constant, Λ the thermal de Broglie wavelength, and $\nu_{\rm id}$ a free parameter introduced in Eq. (2) of Ref. [5] (in the standard theory it is equal to unity). The second term is the repulsive f–f interaction approximated by a hard-sphere (HS) functional taken from Kierlik and Rosinberg (KR) [6], where $d_{\rm HS}$ is the HS diameter. The third term is the attractive f–f interaction treated in a mean field approximation (MFA), which is written in terms of a recently proposed [2] version of the separation of the Lennard–Jones (LJ) potential originally introduced by Weeks, Chandler, and Andersen (WCA) [7]: $\Phi^{\rm WCA}_{\rm attr}(r=|\mathbf{r}-\mathbf{r}'|) = -\tilde{\varepsilon}_{ff}$ for $r \le r_m$ and $\Phi^{\rm WCA}_{\rm attr}(r) = 4\tilde{\varepsilon}_{ff}[(\tilde{\sigma}_{ff}/r)^{12}-(\tilde{\sigma}_{ff}/r)^6]$ for $r > r_m$, where $r_m = 2^{1/6}\tilde{\sigma}_{ff}$ is the position of the LJ minimum. The well depth $\tilde{\varepsilon}_{ff}$ and interaction size $\tilde{\sigma}_{ff}$ are considered as free parameters because the use of its standard bare values $\varepsilon_{\rm XeXe}/k_B = 221$ K and $\sigma_{\rm XeXe} = 0.41$ nm (see, e.g., Refs. [8,9]) overestimates the experimental result for the critical temperature T_c. We set $d_{\rm HS} = \tilde{\sigma}_{ff}$.

The three adjustable parameters (namely, ν_{id}, $\tilde{\varepsilon}_{ff}$, and $\tilde{\sigma}_{ff}$) were determined by imposing that on the liquid–vapor (l–v) coexistence curve of Xe at a fixed T (between the triple point $T_t = 161.3$ K and the critical $T_c = 289.74$ K) the data of $\rho_l(T)$, $\rho_v(T)$, and $P_0(T) = P(\rho_l) = P(\rho_v)$ listed in Table XXIII of Ref. [10] be reproduced and the condition $\mu(\rho_l) = \mu(\rho_v) = \mu_0(T)$ be satisfied.

The equilibrium $\rho(z)$ and μ are obtained from Euler–Lagrange (EL) equations derived by minimizing the free energy with respect to density variation at a fixed number of particles N per unit area of the wall A defined as $N_s = N/A = \int_0^L \rho(z)\, dz$. Here L is the size of the box adopted for solving the E–L equations. Dimensionless variables $z^* = z/\tilde{\sigma}_{ff}$ and $L^* = L/\tilde{\sigma}_{ff}$ for distances, and $N^*_s = N\tilde{\sigma}^2_{ff}/A$ for areal density are used.

* Corresponding author at: Laboratorio TANDAR, Departamento de Física, Comisión Nacional de Energía Atómica, RA-1429 Buenos Aires, Argentina. Tel.: +54 11 6772 7064; fax: +54 11 6772 7121.
E-mail address: szybisz@tandar.cnea.gov.ar (L. Szybisz).

0921-4526/$ - see front matter © 2012 Elsevier B.V. All rights reserved.
doi:10.1016/j.physb.2011.12.086

Before entering into the analysis of physisorption, we evaluated the surface tension of the free liquid–vapor interface, γ_{lv}, by setting $U_{sf}(z)=0$ and following the procedure outlined in previous works [2–4]. Our results agree very well (in a similar way as for Ne and Ar in the latter references) with experimental data [11] over the entire temperature range $T_t \le T \le T_c$.

2. Analysis of the adsorption

For the analysis of physisorption we adopted in all the cases the *ab initio* potentials of Chismeshya, Cole, and Zaremba (CCZ), i.e. we set $U_{sf}(z)=U_{CCZ}(z)$ given by Eq. (3) in Ref. [12] with the potential parameters listed in Table 1 therein (see also the expression in Ref. [9]). In the present work, we report results for adsorption of Xe on surfaces of Cs, Na, Li, and Mg. The corresponding CCZ potentials are plotted in Fig. 1. This set of substrates with $\varepsilon_r = W_{sXe}/\varepsilon_{XeXe} = 1.5$, 2.1, 2.8, and 5.4, respectively, sweeps different wetting scenarios. The EL equations are solved in a box of size $L^* = 40$. Adsorption isotherms at fixed temperatures, i.e. $\Delta\mu = \mu - \mu_0(T)$, were calculated as a function of the excess surface density (coverage), often expressed in nominal layers ℓ as $\Gamma_\ell = (1/\rho_l^{2/3}) \int_0^L dz[\rho(z)-\rho_B]$, where ρ_B is the asymptotic bulk vapor density and ρ_l the liquid density at saturation for a given temperature.

Fig. 2 shows adsorption isotherms for Xe/Cs close to the wetting temperature T_w. One may observe that at $T=270$ K the difference $\Delta\mu$ increases monotonically, while at lower T there are oscillations. At $T=269$ and 268 K an equal area Maxwell construction is feasible, but at $T=267$ K the data do not allow such a construction. A Maxwell construction determines a jump in coverage $\Delta\Gamma_\ell = \Gamma_{\ell,max} - \Gamma_{\ell,min}$ at $\Delta\mu_{pw}(T)$, which is characteristic of the prewetting (PW) phenomenon. At T_w the jump is infinite and its size diminishes for increasing T until its disappearance at the critical PW (CPW) temperature T_{cpw}. Above $\Gamma_{\ell,max}$ the film grows continuously without any further jump in coverage. The temperature dependence of $\Delta\mu_{pw}(T)$ is shown in Fig. 3. This quantity approaches tangentially zero at T_w. From thermodynamic arguments [13] the tangency may be described by the form $\Delta\mu_{pw}(T) = \mu_{pw}(T) - \mu_0(T) = a_{pw}(T-T_w)^{3/2}$. Here a_{pw} is a model parameter and the exponent 3/2 is fixed by the asymptotic form $\sim 1/z^3$ of $U_{sf}(z)$. In practice, this expression is used to fit data of $\Delta\mu_{pw}(T)$ for determining T_w. The Xe/Cs system undergoes to a weak first-order transition at $T_w = 267.5$ K with $a_{pw}/k_B = -0.18\ \mathrm{K}^{-1/2}$. The CPW point at $T_{cpw} \lesssim 270$ K. So, the present DF results indicate that Xe wets Cs. This conclusion is in contradiction with that obtained by Curtarolo et al. [9] from Grand Canonical Monte Carlo (GCMC) simulations. We shall comment this fact below.

Fig. 4 shows the adsorption isotherms for Xe/Na at temperatures above T_w. The PW line is included in Fig. 3. This kind of PW behavior corresponds to the case depicted in panel (b) of Fig. 1 in Ref. [13] and has been measured in several systems [1]. In the

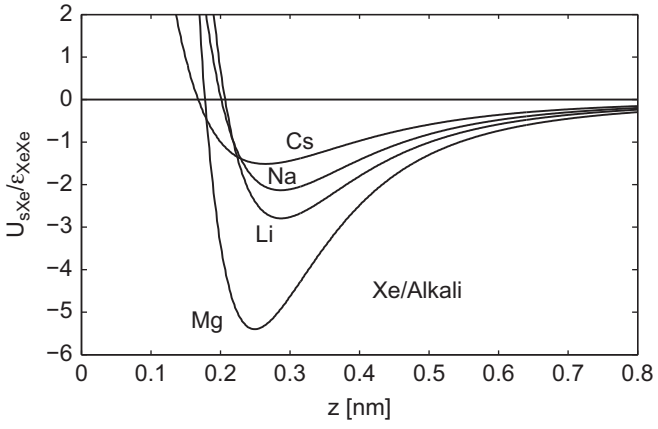

Fig. 1. Comparison of CCZ adsorption potentials for Xe taken from Ref. [12]. Data are normalized to ε_{XeXe} and identified for each substrate.

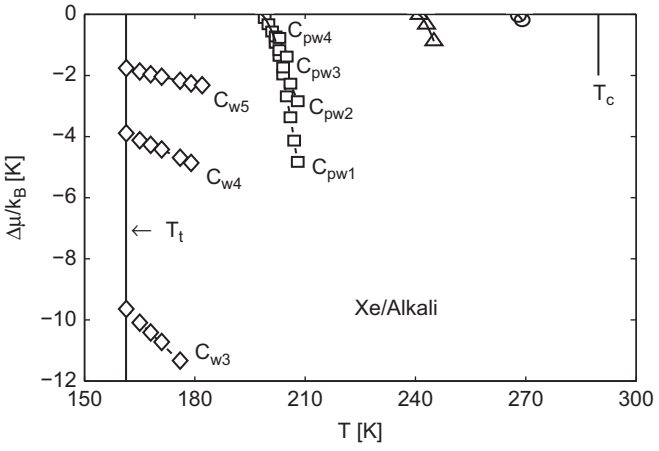

Fig. 3. Prewetting lines for Xe adsorbed on Cs (circles), Na (up-triangles), Li (squares), and Mg (diamonds). Data are delimited by T_t an T_c.

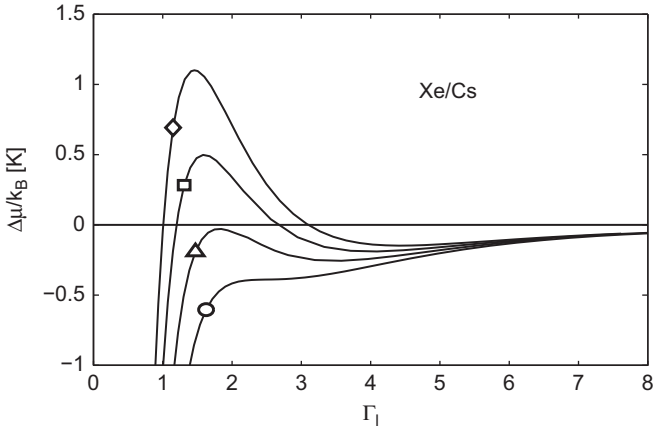

Fig. 2. Adsorption isotherms for the Xe/Cs system evaluated at $T=267$ K (diamond), 268 K (square), 269 K (up-triangle), and 270 K (circle).

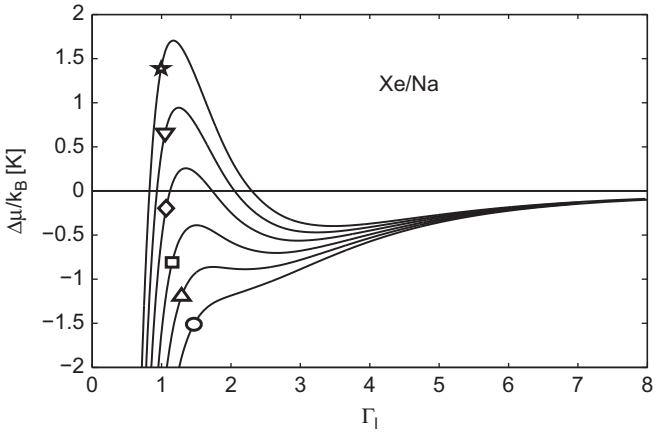

Fig. 4. Same as Fig. 2 but for Xe/Na at $T=241$ K (star), 242 K (down-triangle), 243 K (diamond), 244 K (square), 245 K (up-triangle), and 246 K (circle).

case of Xe/Na we obtained T_w=240.8 K and $a_{pw}/k_B = -0.10\ \mathrm{K}^{-1/2}$. In addition, Fig. 4 fixes an upper limit for the CPW point at $T_{cpw} \lesssim 246$ K.

Adsorption isotherms for the Xe/Li system are displayed in Fig. 5. In this case, equal area Maxwell constructions yield multiple jumps in coverage at a fixed T. In turn, this feature leads to the series of PW lines (C_{pw1}, C_{pw2}, C_{pw3}, and C_{pw4}) plotted in Fig. 3, where one may observe that for decreasing temperature all of them coalesce into one curve. This behavior corresponds to that of panel (d) in Fig. 1 of Ref. [13]. The tangential fit of the line of coalescence yielded T_w=198.0 K and $a_{pw}/k_B = -0.11\ \mathrm{K}^{-1/2}$. The present T_w almost coincides with T_w=201 K predicted by a rather crude simple model, see Table 1 in Ref. [12], but is lower than the value T_w=225 K quoted in Table I of [8] obtained from GCMC calculations.

It is hard to explain the qualitative difference between the present DF and the GCMC calculations of Ref. [8], because usually the GCMC results are taken as reference values. In this context, it becomes important to notice the failure of these GCMC simulations in reproducing the measured wetting of Rb by Ne [14] (see Table I in Ref. [8]), while our calculations [2] agree with that experimental result (see also discussions in Refs. [4,18]).

Adsorption isotherms calculated for Xe/Mg at $T = T_t$, $T_{nb} = 165.03$ K (normal boiling temperature), 171 K, 176 K, and 182 K are displayed in Fig. 6. These data do not exhibit a "standard" PW pattern because Mg is significantly more attractive than the alkali metals. A layer-by-layer film growth for $T \geq T_t$ may be observed. The phase diagram for the 3th (C_{w3}), 4th (C_{w4}), and 5th (C_{w5}) layer is shown in Fig. 3 (the scale of this drawing unable us to plot results for the first two layers), this behavior is similar to that depicted in Fig. 16(a) of Ref. [15] for strong substrates.

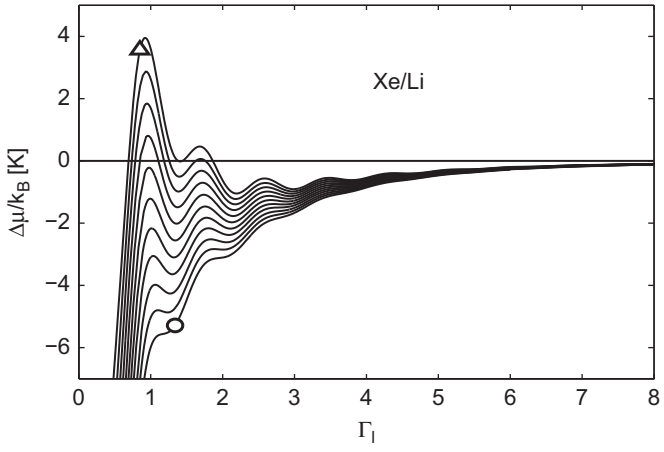

Fig. 5. Same as Fig. 2 but for Xe/Li at temperatures from T=199 K (up-triangle) to 209 K (circle), with a step $\Delta T = 1$ K.

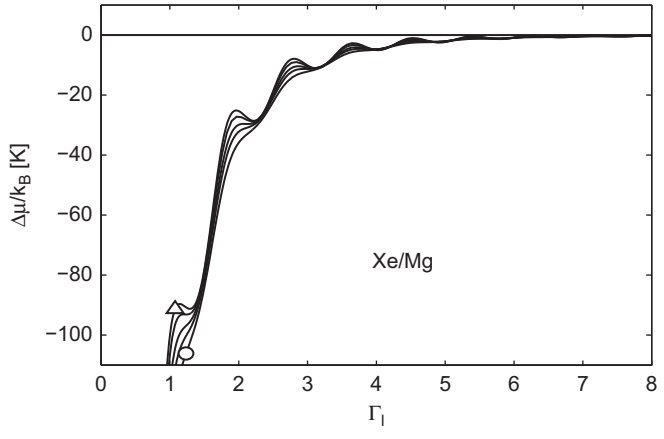

Fig. 6. Same as Fig. 2 but for Xe/Mg at temperatures from $T = T_t$ (up-triangle) to 182 K (circle).

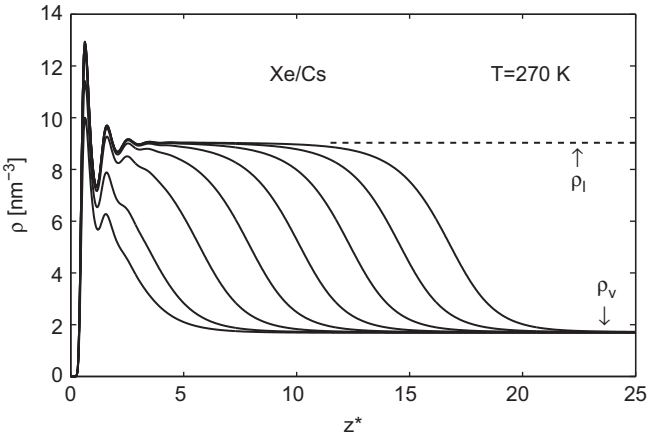

Fig. 7. Density profiles of Xe adsorbed on a single wall of Cs at T=270 K for increasing coverages from $\Gamma_\ell = 1.221$ to 11.099. Quantities ρ_l and ρ_v are the liquid and vapor equilibrium densities at the coexistence curve for the given temperature.

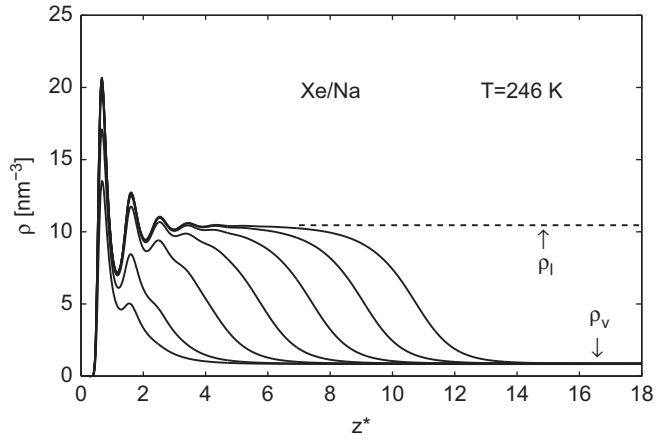

Fig. 8. Same as Fig. 7 for Xe/Na at T=246 K for Γ_ℓ from 0.873 to 8.844.

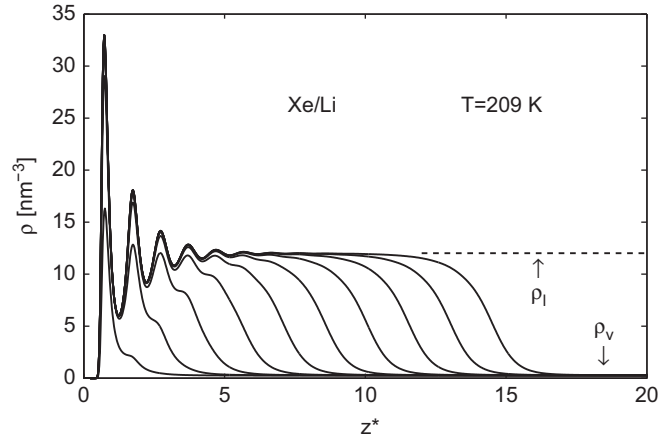

Fig. 9. Same as Fig. 7 for Xe/Li at T=209 K for $\Gamma_\ell = 0.556$ and 11.874.

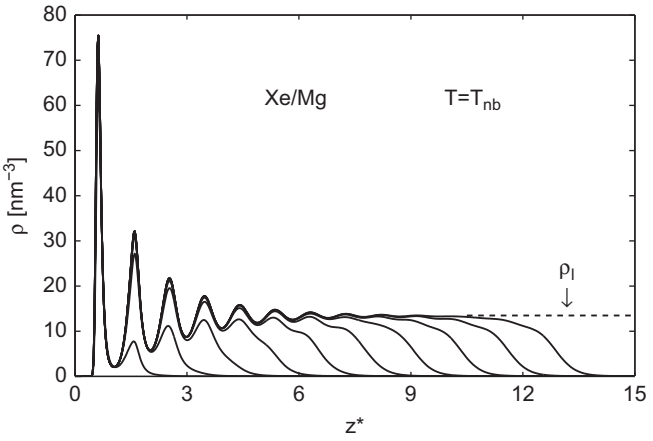

Fig. 10. Same as Fig. 7 for Xe/Mg at $T = T_{nb}$ for coverages from $\Gamma_\ell = 1.107$ to 11.638.

Figs. 7–9 show the continuous growth of adsorbed Xe on substrates of Cs, Na, and Li at temperatures just above the corresponding T_{cpw}, and Fig. 10 shows the same feature for Mg at T_{nb}. In all the cases, after a layered regime the liquid profile stabilizes at the equilibrium bulk liquid density, ρ_l, at the given T. Next, the density falls off reaching the equilibrium bulk vapor density, ρ_v. In addition, one may observe that ratio of the first layer's peak ρ_{1-peak} over ρ_l increases for increasing ε_r. For Mg one gets $\rho_{1-peak}/\rho_l \approx 5$, which is only slightly larger than the ratio found for the deposition of Xe on surfaces of Al, see Fig. 2C in Ref. [19]. The density of the latter "rather" two-dimensionally confined liquids is much larger than that of the compressed solid Xe, $\rho_s \simeq 20\,\mathrm{nm}^{-3}$ [10]. On the other hand, the density at the first valley of these structures is sizable smaller than ρ_l.

3. Summary

The adsorption of Xe on structureless planar substrates of Cs, Na, Li, and Mg, with increasing values of $\epsilon_r (= W_{sf}/\varepsilon_{ff})$ exhibits a rich variety of wetting scenarios. For the present DF calculations we used realistic f–f and s–f interactions. Properties of the obtained adsorption isotherms and density profiles indicate a route for getting very dense first layers. The evolution from "normal" liquid first layers toward "highly" compressed ones is illustrated by the sequence of Figs. 7–10. This behavior may be correlated with the features shown in Fig. 3, where the information contained in the series of adsorption isotherms is summarized. In order to get a better insight of the nature of these structures, we are planning to apply DF devised for describing the adsorption of solid structures. A pioneering attempt to formulate a DF for solid has been reported by Tarazona [16] and a review has been recently published by Roth [17].

References

[1] M.S. Petersen, M.W. Cole (Guest Eds.), J. Low Temp. Phys. 157 (2009) 75 (Special Issue: Wetting, Spreading and Filling).
[2] S.A. Sartarelli, L. Szybisz, I. Urrutia, Phys. Rev. E 79 (2009) 011603.
[3] S.A. Sartarelli, L. Szybisz, Papers Phys. 1 (2009) 010001. 〈also at http://arxiv.org/abs/0909.2244〉.
[4] S.A. Sartarelli, L. Szybisz, Phys. Rev. E 80 (2009) 052602.
[5] F. Ancilotto, S. Curtarolo, F. Toigo, M.W. Cole, Phys. Rev. Lett. 87 (2001) 206103.
[6] E. Kierlik, M.L. Rosinberg, Phys. Rev. A 42 (1990) 3382.
[7] J.D. Weeks, D. Chandler, H.C. Andersen, J. Chem. Phys. 54 (1971) 5237.
[8] S. Curtarolo, G. Stan, M.J. Bojan, M.W. Cole, W.A. Steele, Phys. Rev. E 61 (2000) 1670.
[9] S. Curtarolo, M.W. Cole, R.D. Diehl, Phys. Rev. B 70 (2004) 115403.
[10] V.A. Rabinovich, A.A. Vasserman, V.I. Nedostup, L.S. Veksler, Thermophysical Properties of Neon, Argon, Krypton, and Xenon, Hemisphere, Washington, DC, 1988.
[11] B.L. Smith, P.R. Gardner, E.H.C. Parker, J. Chem. Phys. 47 (1967) 1148; J. Zollweg, G. Hawkins, G.B. Benedek, Phys. Rev. Lett. 27 (1971) 1182.
[12] A. Chizmeshya, M.W. Cole, E. Zaremba, J. Low Temp. Phys. 110 (1998) 677.
[13] R. Pandit, M.E. Fisher, Phys. Rev. Lett. 51 (1983) 1772.
[14] G.B. Hess, M.J. Sabatini, M.H.W. Chan, Phys. Rev. Lett. 78 (1997) 1739.
[15] R. Pandit, M. Schick, M. Wortis, Phys. Rev. B 26 (1982) 5112.
[16] P. Tarazona, Mol. Phys. 52 (1984) 81; P. Tarazona, Phys. Rev. A 31 (1985) 2672.
[17] R. Roth, J. Phys.: Condens. Matter 22 (2010) 063102.
[18] M. Zeng, J. Mi, C. Zhong, Phys. Rev. B 82 (2010) 125452.
[19] S.E. Donnelly, et al., Science 296 (2002) 507.